INTERNATIONAL JOURNAL OF
NUMERICAL ANALYSIS AND MODELING
Volume 20, Number 4, Pages 459–477

doi: 10.4208/ijnam2023-1019

UNCONDITIONAL ENERGY STABILITY AND SOLVABILITY FOR A C0 INTERIOR PENALTY METHOD FOR A SIXTH-ORDER EQUATION MODELING MICROEMULSIONS

AMANDA E. DIEGEL AND NATASHA S. SHARMA*

Abstract. We consider a C0 interior penalty finite element approximation of a sixth-order Cahn-Hilliard type equation that models the dynamics of phase transitions in ternary oil-water-surfactant systems. The nonlinear sixth-order parabolic equation is expressed in a mixed form whereby a second-order (in space) parabolic equation and an algebraic fourth-order (in space) nonlinear equation are considered. The temporal discretization is chosen so that a discrete energy law can be established leading to unconditional energy stability. Additionally, we show that the numerical method is unconditionally uniquely solvable. We conclude with several numerical experiments demonstrating the unconditional stability and first-order accuracy of the proposed method.

Key words. Finite element, Cahn-Hilliard, unconditional energy stability, microemulsions and unique solvability.

1. Introduction

Microemulsion systems are of great interest across many different fields due to the flexibility of these models to adapt to a variety of applications such as oil recovery [2], development of environment-friendly solvents [1], consumer and commercial cleaning product formulations [3], and drug delivery systems [4]. One such model, which is outlined below, can be described as a sixth-order conserved evolution system that models the dynamics of phase transitions in ternary oil-water-surfactant systems. This model was introduced and studied by Gompper and co-authors in [5, 6, 7, 8, 9] and has demonstrated great ability in capturing many essential static properties of the ternary oil-water-surfactant systems. The existence and uniqueness of strong and weak solutions have been analyzed by Pawlow et al. in [10, 11].

Assume that $\Omega \subset \mathbb{R}^2$ is a bounded polygonal domain occupied by the oil-water-surfactant mixture with boundary $\partial\Omega$. Then, according to Gompper [9], the free energy functional assumes the form

$$E(\phi) = \int_\Omega f_0(\phi)\ dx + \frac{1}{2}\int_\Omega \left\{(\phi^2 - a_0)|\nabla\phi|^2 + \lambda(\Delta\phi)^2\right\}\ dx, \tag{1}$$

where ϕ is the scalar order parameter representing the local difference between oil and water concentrations and a_0 and λ are positive constants. Here, $f_0(\phi)$ denotes the volumetric nonlinear free energy functional which has the form

$$f_0(\phi) = \frac{\beta}{2}(\phi-1)^2(\phi^2+0.5)(\phi+1)^2 = \frac{\beta}{2}\Big(\phi^6 - 1.5\phi^4 + 0.5\Big),$$

and possesses three extrema at $\phi = \pm 1,\ 0$ which correspond to the water-rich (-1), oil-rich (+1), and microemulsion (0) phases. We note that while this model

Received by the editors on September 7, 2022 and, accepted on March 7, 2023.
2000 *Mathematics Subject Classification.* 65M60, 74N20, 74S05.
*Corresponding author.

is defined for an arbitrary choice of a_0, in this paper, we limit the range of a_0 to positive numbers. The impact of a_0 can be explained as follows. When the surfactant is added to the system, a minimum develops in the microemulsion phase which is represented by $\phi = 0$. The minimum is of value $-a_0$. When surfactant concentration is increased, the phase field ϕ satisfies $\phi^2 < a_0$. For a detailed discussion, we direct the interested reader to [10] and references therein.

To construct a system of equations representing the dynamics of phase transitions in ternary oil-water-surfactant systems, we follow Pawlow and Zajaczkowski [10] and assume the initial value condition

$$\phi(0) = \phi_0 \in H^4(\Omega) \text{ such that } \mathbf{n} \cdot \nabla\phi_0 = \mathbf{n} \cdot \nabla\Delta\phi_0 = 0 \text{ on } \partial\Omega, \tag{2}$$

and homogeneous Neumann-type boundary conditions

$$\mathbf{n} \cdot \nabla\phi = \mathbf{n} \cdot \nabla\Delta\phi = \mathbf{n} \cdot \nabla\mu = 0. \tag{3}$$

Additionally, we consider the following conservation law

$$\partial_t\phi - \nabla \cdot (\mathcal{M}\nabla\mu) = 0, \tag{4}$$

where $\mathcal{M} > 0$ is a constant mobility and μ is the chemical potential given by $\delta_\phi E$, i.e. the variational derivative of the energy functional E with respect to ϕ:

$$\mu := \delta_\phi E = 3\beta(\phi^5 - \phi^3) + \phi|\nabla\phi|^2 - \nabla \cdot ((\phi^2 - a_0)\nabla\phi) + \lambda\Delta^2\phi. \tag{5}$$

Therefore, we consider the following system of equations for which the well-posedness was established in [10]:

$$\partial_t\phi - \nabla \cdot (\mathcal{M}\nabla\mu) = 0, \tag{6a}$$

$$3\beta(\phi^5 - \phi^3) + \phi|\nabla\phi|^2 - \nabla \cdot ((\phi^2 - a_0)\nabla\phi) + \lambda\Delta^2\phi - \mu = 0. \tag{6b}$$

The following theorem establishes the energy stability of the above system.

Theorem 1.1. *Let ϕ be a sufficiently regular solution to the system* (6)*. Then, for $t \geq 0$, the following equality holds.*

$$\frac{d}{dt}\Big(\int_\Omega f_0(\phi)\ dx + \frac{1}{2}\int_\Omega \left\{(\phi^2 - a_0)|\nabla\phi|^2 + \lambda(\Delta\phi)^2\right\}\ dx\Big) + \ \mathcal{M}\int_\Omega |\nabla\mu|^2\, dx = 0.$$

Proof. The proof can be found in Lemma 3.1 from [10]. □

Despite its popularity, there has been a lack of available numerical schemes solving these systems. Indeed, the only established numerical method developed for the model (6) known to the authors was introduced by Hoppe and Linsenmann in [12] in which a C^0 interior penalty (C0-IP) method was utilized for spacial discretization but where a fully implicit backward Euler time discretization strategy was adopted for the error analysis. As such, the work presented in that paper focuses on establishing quasi-optimal error estimates but no discrete energy law is obtained.

Similar to the work presented in [12], we propose a spacial discretization based on the C0-IP method. These methods are characterized by the use of C^0 Lagrange finite elements where C^1 continuity requirements imposed by utilizing a conforming mesh are replaced with interior penalty techniques. C0-IP methods were first introduced by G. Engel et.al. in [13] and revisited and analyzed by Brenner et.al. in [14, 15, 16, 17, 18, 19, 20, 21, 22, 23, 24] and further investigated by others in [25] and [26] to solve the fourth-order biharmonic problem. However, in contrast to the work presented by Hoppe and Linsenmann, we propose a time discretization strategy from which a discrete energy law closely related to (1) is satisfied by solutions to

the numerical scheme. We also provide details for the proof for unique solvability. Closely related work by the authors of this paper on a sixth-order parabolic equation modeling the phase-field crystal (PFC) equation can be found in [28] and due to the success of that implementation, the authors have chosen the C0-IP approach herein. However, it may be worthwhile to remark that other available numerical methods for the PFC equation have recently emerged in the literature and include a local discontinuous Galerkin method by Guo and Xu [27], a Scalar Auxiliary Variable Fourier-spectral method by Li and Shen [29], and an Invariant Energy Quadratization approach by Yang and Han [37]. Consideration of adopting a numerical approach differing from the C0-IP method for the microemulsions system is reserved for future work. Additionally, extensive numerical tests are conducted to demonstrate the stability and the first-order accuracy of the scheme proposed herein.

This paper is organized as follows. We first present preliminaries in section 2 which will be required for the definition of the C0-IP method. In section 3, we present the fully discrete C0-IP method and demonstrate that this method is unconditionally uniquely solvable and unconditionally stable. In section 4, we present several numerical experiments illustrating the performance of our method and conclude the paper in section 5.

2. Preliminaries

Suppose that $\mathscr{T}_h$ is a geometrically conforming simplicial triangulation of Ω. We introduce the following notation:

- h_K = diameter of triangle K ($h = \max_{K\in\mathscr{T}_h} h_K$),
- v_K = restriction of the function v to the triangle K,
- $|K|$ = area of the triangle K,
- $\mathscr{E}_h$ = the set of the edges of the triangles in $\mathscr{T}_h$,
- e = the edge of a triangle,
- $|e|$ = the length of the edge,
- $V_h := \{w_h \in C(\overline{\Omega}) | (w_h)_K \in P_1(K)\ \forall K \in \mathscr{T}_h\}$ the standard Lagrange finite element spaces associated with $\mathscr{T}_h$ of degree 1.
- $Z_h := \{v_h \in C(\overline{\Omega}) | (v_h)_K \in P_2(K)\ \forall K \in \mathscr{T}_h\}$ the standard Lagrange finite element space associated with $\mathscr{T}_h$ of degree 2.

We rely on the standard Sobolev space, inner product, and norm notation for the remainder of this paper. In particular, for $1 < p < \infty$ we let $\|\cdot\|_{L^p(S)}$ denote the standard L^p norm over $S \subset \mathbb{R}^2$ and for $S = \Omega$, we denote the L^p norm by simply $\|\cdot\|_{L^p}$. Additionally, we define the bilinear form:

$$
\begin{aligned}
a_h^{IP}(w,v) := &\sum_{K\in\mathscr{T}_h}\int_K \left(\nabla^2 w : \nabla^2 v\right) dx + \sum_{e\in\mathscr{E}_h}\int_e \left\{\left\{\frac{\partial^2 w}{\partial n_e^2}\right\}\right\}\left[\!\left[\frac{\partial v}{\partial n_e}\right]\!\right] dS \\
&+ \sum_{e\in\mathscr{E}_h}\int_e \left\{\left\{\frac{\partial^2 v}{\partial n_e^2}\right\}\right\}\left[\!\left[\frac{\partial w}{\partial n_e}\right]\!\right] dS + \alpha\sum_{e\in\mathscr{E}_h}\frac{1}{|e|}\int_e \left[\!\left[\frac{\partial w}{\partial n_e}\right]\!\right]\left[\!\left[\frac{\partial v}{\partial n_e}\right]\!\right] dS,
\end{aligned} \tag{7}
$$

with $\alpha \geq 1$ known as a penalty parameter and $\left(\nabla^2 u : \nabla^2 v\right)$ is the inner product of the Hessian matrices of u and v. The jumps and averages that appear in (7) are defined as follows. For an interior edge e shared by two triangles $K_\pm$ where n_e points from K_- to K_+ (cf. Figure 1), we define on the edge e

$$
\left[\!\left[\frac{\partial v}{\partial n_e}\right]\!\right] = n_e \cdot \left(\nabla v_+ - \nabla v_-\right), \quad \left\{\left\{\frac{\partial^2 v}{\partial n_e^2}\right\}\right\} = \frac{1}{2}\left(\frac{\partial^2 v_-}{\partial n_e^2} + \frac{\partial^2 v_+}{\partial n_e^2}\right), \tag{8}
$$

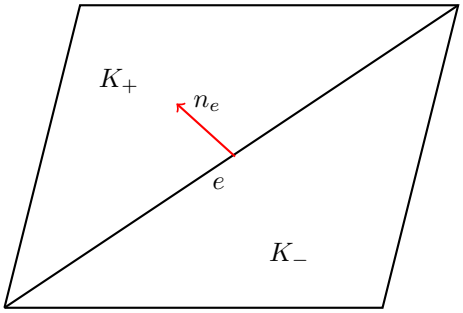

FIGURE 1. Orientation of the unit normal n_e outward to the interior triangle K_-. This normal is defined on the interface e shared by the triangles K_- and K_+.

where $v_\pm = v|_{K_\pm}$. For a boundary edge e, we take n_e to be the unit normal pointing towards the outside of Ω and define on the edge e

$$\left[\!\left[\frac{\partial v}{\partial n_e}\right]\!\right] = -n_e \cdot \nabla v_K, \quad \left\{\!\left\{\frac{\partial^2 v}{\partial n_e^2}\right\}\!\right\} = n_e \cdot \left(\nabla^2 v\right) n_e. \tag{9}$$

Remark 2.1. *Note that the definitions* (8) *and* (9) *are independent of the choice of $K_\pm$, or equivalently, independent of the choice of n_e.*

The accuracy of the C0-IP method is measured by the mesh-dependent norm

$$\|v_h\|_{2,h}^2 := \sum_{K\in\mathscr{T}_h} |v_h|_{H^2(K)}^2 + \sum_{e\in\mathscr{E}_h} \frac{\alpha}{|e|} \left\| \left[\!\left[\frac{\partial v_h}{\partial n_e}\right]\!\right] \right\|_{L^2(e)}^2, \tag{10}$$

where the seminorm $|w_h|_{H^2(K)}$ is defined by $|w_h|_{H^2(K)}^2 = \int_K \left(\nabla^2 w_h : \nabla^2 w_h\right) dx$. The following lemma guarantees the boundedness of $a_h^{IP}(\cdot,\cdot)$.

Lemma 2.1 (Boundedness of $a_h^{IP}(\cdot,\cdot)$)**.** *There exists positive constants C_{cont} and C_{coer} such that for choices of the penalty parameter α large enough we have*

$$a_h^{IP}(w_h, v_h) \le C_{cont} \|w_h\|_{2,h} \|v_h\|_{2,h} \quad \forall\, w_h, v_h \in Z_h, \tag{11}$$

$$C_{coer} \|w_h\|_{2,h}^2 \le a_h^{IP}(w_h, w_h) \quad \forall\, w_h \in Z_h, \tag{12}$$

where the constants C_{cont} and C_{coer} depend only on the shape regularity of $\mathscr{T}_h$.

Proof. See [14]. □

We remark that for all $v \in Z_h$, we have the following Poincaré type inequalities: There exists a constant C_P depending only on Ω such that,

$$\|v\|_{L^2} \le C_P \|\nabla v\|_{L^2} \quad \text{and} \quad \|\nabla v\|_{L^2} \le C_P \|v\|_{2,h}. \tag{13}$$

Additionally, the first of these inequalities hold for all $v \in H_N^2(\Omega)$, where $H_N^2(\Omega) = \{z \in H^2(\Omega) | \mathbf{n}\cdot\nabla z = 0 \text{ on } \partial\Omega\}$. Finally, we present a lemma that provides a method for bounding $|(\nabla w_h, \nabla v)|$ where $w_h \in Z_h$ and $v \in H^1(\Omega)$.

Lemma 2.2. *Suppose Ω is a bounded polygonal domain. For all $w_h \in Z_h, v \in H^1(\Omega)$ and α large enough,*

$$|(\nabla w_h, \nabla v)| \le \sqrt{2} \|w_h\|_{2,h} \|v\|_{L^2}. \tag{14}$$

Proof. See [30] for the proof. □

The remainder of the preliminaries will help in proving the existence of solutions to the fully-discrete numerical method. Therefore, we define the spaces

$$\mathring{V}_h = V_h \cap L^2_0(\Omega) \quad \text{and} \quad \mathring{Z}_h = Z_h \cap L^2_0(\Omega),$$

where $L^2_0(\Omega)$ is the space of square-integrable functions with zero mean. Additionally, we define an invertible linear operator $\mathsf{T}_h : \mathring{Z}_h \to \mathring{Z}_h$ via the variational problem: given $\zeta \in \mathring{Z}_h$, find $\mathsf{T}_h(\zeta) \in \mathring{Z}_h$ such that

$$(\nabla \mathsf{T}_h(\zeta_h), \nabla \chi_h) = (\zeta_h, \chi_h) \qquad \forall\, \chi_h \in \mathring{Z}_h. \tag{15}$$

Remark 2.1. *The variational problem used to define the linear operator T_h clearly has a unique solution due to the fact that $(\nabla\cdot, \nabla\cdot)$ is an inner product on $\mathring{Z}_h$.*

The following properties related to the linear operator T_h have been established in [31]. Let ζ_h, $\xi_h \in \mathring{Z}_h$ and set

$$(\zeta_h, \xi_h)_{-1,h} := (\nabla \mathsf{T}_h(\zeta_h), \nabla \mathsf{T}_h(\xi_h)) = (\zeta_h, \mathsf{T}_h(\xi_h)) = (\mathsf{T}_h(\zeta_h), \xi_h)\,. \tag{16}$$

The definition of $(\,\cdot\,,\,\cdot\,)_{-1,h}$ above defines an inner product on $\mathring{Z}_h$, and the induced negative norm satisfies

$$\|\zeta_h\|_{-1,h} := \sqrt{(\zeta_h, \zeta_h)_{-1,h}} = \sup_{0 \neq \chi_h \in Z_h} \frac{(\zeta_h, \chi_h)}{\|\nabla \chi_h\|_{L^2}}. \tag{17}$$

Consequently, for all $\chi_h \in Z_h$ and all $\zeta_h \in \mathring{Z}_h$,

$$|(\zeta_h, \chi_h)| \leq \|\zeta_h\|_{-1,h} \|\nabla \chi_h\|_{L^2}\,. \tag{18}$$

The following Poincaré-type estimate holds:

$$\|\zeta_h\|_{-1,h} \leq C \|\zeta_h\|_{L^2}\,, \quad \forall\, \zeta_h \in \mathring{Z}_h, \tag{19}$$

for some $C > 0$ that is independent of h. Finally, if $\mathscr{T}_h$ is globally quasi-uniform, then the following inverse estimate holds:

$$\|\zeta_h\|_{L^2} \leq C h^{-1} \|\zeta_h\|_{-1,h}\,, \quad \forall\, \zeta_h \in \mathring{Z}_h, \tag{20}$$

for some $C > 0$ that is independent of h.

3. The Fully-Discrete C0-IP Method

We begin with a description of the time stepping strategy. Let M be a positive integer such that $t_m = t_{m-1} + \tau$ for $1 \leq m \leq M$ where $t_0 = 0$, $t_M = T$ with $\tau = T/M$. Additionally, denote by ϕ^m an approximation of ϕ at time t_m and define the numerical time derivative as $\delta_\tau \phi^m := \frac{\phi^m - \phi^{m-1}}{\tau}$. The time discretization strategy can be described as follows: a convex-splitting treatment of the volumetric nonlinear free energy functional $f_0(\phi)$ is chosen and the treatment of the problematic nonlinear term $\phi^2|\nabla\phi|^2$ in (6b) follows a discretization such that a discrete product rule is guaranteed. Therefore, using the notations and definitions defined in Section 2, the fully-discrete finite element method for (6a)–(6b) is stated as follows: Given $\phi_h^{m-1} \in Z_h$, find $(\phi_h^m, \mu_h^m) \in Z_h \times V_h$ which satisfies

$$(\delta_\tau \phi_h^m, \nu_h) + (\mathcal{M} \nabla \mu_h^m, \nabla \nu_h) = 0, \qquad \forall \quad \nu_h \in V_h \tag{21a}$$

$$\begin{aligned} &3\beta \left((\phi_h^m)^5 - (\phi_h^{m-1})^3, \psi_h\right) + \left((\phi_h^m)^2 \nabla \phi_h^m, \nabla \psi_h\right) + \left(\phi_h^m |\nabla \phi_h^{m-1}|^2, \psi_h\right) \\ &-a_0 \left(\nabla \phi_h^{m-1}, \nabla \psi_h\right) + \lambda\, a_h^{IP}\left(\phi_h^m, \psi_h\right) - \left(\mu_h^m, \psi_h\right) = 0 \qquad \forall \quad \psi_h \in Z_h, \end{aligned} \tag{21b}$$

where the initial data is taken to be $\phi_h^0 := P_h \phi_0 = P_h \phi(0)$ such that $P_h : H^2_N(\Omega) \to Z_h$ is a projection operator which can either be a nodal interpolation or an elliptic projection operator.

Remark 3.1. *The scheme* (21) *satisfies the discrete conservation property* $(\phi_h^m, 1) = \left(\phi_h^0, 1\right) = (\phi_0, 1)$ *for any* $1 \leq m \leq M$. *This can be shown by choosing* $\nu_h \equiv 1$ *in* (21a). *The quantity* $\frac{1}{|\Omega|}(\phi_0, 1)$ *is referred to as the average of* ϕ_0 *over* Ω *and is denoted by* $\overline{\phi}_0$. *Due to the discrete conservation property, it follows that* $(\phi_h^m, 1) = \left(\phi_h^0, 1\right) = |\Omega|\,\overline{\phi}_0$.

3.1. Existence of a Solution. We are now in a position to prove the existence of a solution to (21).

Lemma 3.1. *Let* $\varphi_h^{m-1} \in \mathring{Z}_h$ *be given and let* $\lambda \geq \dfrac{3\beta|\overline{\phi}_0|^4 C_{P,1}}{C_{coer}}$, *where* $C_{P,1}$ *depends upon a Poincaré constant but does not depend upon* h *or* τ. *Then, there exists a solution* $(\phi_h^m, \mu_h^m) \in Z_h \times V_h$ *to* (21).

Proof. Let $\varphi_h^{m-1} \in \mathring{Z}_h$ be given and define $\mathscr{G}_h : \mathring{Z}_h \to \mathring{Z}_h$ to be the continuous map such that

$$\begin{aligned}(\mathscr{G}_h(\varphi_h^m), \chi) = \; & 6\beta\tau\left((\varphi_h^m + \overline{\phi_0})^5 - (\varphi_h^{m-1} + \overline{\phi_0})^3, \chi\right) \\ & + 2\tau\left((\varphi_h^m + \overline{\phi}_0)|\nabla\varphi_h^{m-1}|^2, \chi\right) + \; 2\tau\left((\varphi_h^m + \overline{\phi_0})^2\nabla\varphi_h^m, \nabla\chi\right) \\ & - 2a_0\tau\left(\nabla\varphi_h^{m-1}, \nabla\chi\right) + 2\tau\lambda\, a_h^{IP}\left(\varphi_h^m, \chi\right) + \; \frac{2}{\mathcal{M}}\left(\varphi_h^m - \varphi_h^{m-1}, \chi\right)_{-1,h}. \end{aligned} \tag{22}$$

It is a well-known consequence of Brouwer's fixed-point theorem [32] that $\mathscr{G}_h(\varphi_h^m) = 0$ has a solution $\varphi_h^m \in B_q = \{\chi \in \mathring{Z}_h : \|\chi\|_{-1,h} \leq q\}$ if $(\mathscr{G}_h(\chi), \chi) > 0$ for $\|\chi\|_{-1,h} = q$, where we define

$$\begin{aligned} q^2 = & \frac{2\mathcal{M}C_P^4\tau^2}{C_{coer}\lambda}\left\|3\beta\left(\varphi_h^{m-1} + \overline{\phi}_0\right)^3 - \overline{\phi}_0|\nabla\varphi_h^{m-1}|^2\right\|_{L^2}^2 + \frac{2\mathcal{M}C_P^2 a_0^2\tau^2}{C_{coer}\lambda}\left\|\varphi_h^{m-1}\right\|_{L^2}^2 \\ & + \; \left\|\varphi_h^{m-1}\right\|_{-1,h}^2. \end{aligned}$$

Additionally, by the definition of $(\cdot,\cdot)_{-1,h}$, φ_h^m is a solution to $\mathscr{G}_h(\varphi_h^m) = 0$ if and only if it is a solution to

$$\begin{aligned} & 3\beta\left((\varphi_h^m + \overline{\phi_0})^5 - (\varphi_h^{m-1} + \overline{\phi_0})^3, \mathring{\psi}_h\right) + \left((\varphi_h^m + \overline{\phi}_0)|\nabla\varphi_h^{m-1}|^2, \mathring{\psi}_h\right) \\ & \quad + \left((\varphi_h^m + \overline{\phi_0})^2\nabla\varphi_h^m, \nabla\mathring{\psi}_h\right) - a_0\left(\nabla\varphi_h^{m-1}, \nabla\mathring{\psi}_h\right) \\ & \quad\quad + \lambda\, a_h^{IP}\left(\varphi_h^m, \mathring{\psi}_h\right) - \left(\mu_{h,\star}^m, \mathring{\psi}_h\right) = 0, \end{aligned} \tag{23}$$

for all $\mathring{\psi}_h \in \mathring{Z}_h$, where $\mu_{h,\star}^m \in \mathring{V}_h$ is a solution to

$$\left(\mathcal{M}\nabla\mu_{h,\star}^m, \nabla\mathring{\nu}_h\right) = -\left(\frac{\varphi_h^m - \varphi_h^{m-1}}{\tau}, \mathring{\nu}_h\right), \qquad \forall \quad \mathring{\nu}_h \in \mathring{V}_h. \tag{24}$$

By setting $\phi_h^m = \varphi_h^m + \overline{\phi_0}$ and $\mu_h^m = \mu_{h,\star}^m + \overline{\mu_h^m}$, where $\overline{\phi_0}$ is the initial mass average and

$$\overline{\mu_h^m} := \frac{1}{|\Omega|}\left(\overline{\phi_0}|\nabla\varphi_h^{m-1}|^2 + 3\beta(\varphi_h^m + \overline{\phi_0})^5 - 3\beta(\varphi_h^{m-1} + \overline{\phi_0})^3, 1\right), \tag{25}$$

one finds that $(\varphi_h^m, \mu_{h,\star}^m) \in \mathring{Z}_h \times \mathring{V}_h$ is a solution to (23)–(24) if and only if $(\phi_h^m, \mu_h^m) \in Z_h \times V_h$ is a solution to (21).

It therefore remains to be shown that $(\mathscr{G}_h(\chi), \chi) > 0$ for $\|\chi\|_{-1,h} = q$. Using the

polarization identity and Young's inequality, we have

$$\begin{aligned}
&-2\tau\left(3\beta\left(\varphi_h^{m-1}+\overline{\phi_0}\right)^3-\overline{\phi}_0|\nabla\varphi_h^{m-1}|^2,\chi\right)\\
&\quad=-2\left(\frac{C_P^2\sqrt{2}\tau}{\sqrt{C_{coer}\lambda}}\left[3\beta\left(\varphi_h^{m-1}+\overline{\phi_0}\right)^3-\overline{\phi}_0|\nabla\varphi_h^{m-1}|^2\right],\frac{\sqrt{C_{coer}\lambda}}{C_P^2\sqrt{2}}\chi\right)\\
&\quad\geq-\frac{2C_P^4\tau^2}{C_{coer}\lambda}\left\|3\beta\left(\varphi_h^{m-1}+\overline{\phi_0}\right)^3-\overline{\phi}_0|\nabla\varphi_h^{m-1}|^2\right\|_{L^2}^2-\frac{C_{coer}\lambda}{2C_P^4}\|\chi\|_{L^2}^2,\\
&\quad\geq-\frac{2C_P^4\tau^2}{C_{coer}\lambda}\left\|3\beta\left(\varphi_h^{m-1}+\overline{\phi}_0\right)^3-\overline{\phi}_0|\nabla\varphi_h^{m-1}|^2\right\|_{L^2}^2-\frac{C_{coer}\lambda}{2}\|\chi\|_{2,h}^2,
\end{aligned}$$

where C_P is the Poincaré constant from (13). Similarly,

$$-2a_0\tau\left(\nabla\varphi_h^{m-1},\nabla\chi\right)\geq-\frac{2C_P^2a_0^2\tau^2}{C_{coer}\lambda}\left\|\varphi_h^{m-1}\right\|_{L^2}^2-\frac{C_{coer}\lambda}{2}\|\chi\|_{2,h}^2,$$

and

$$\frac{2}{\mathcal{M}}\left(\chi-\varphi_h^{m-1},\chi\right)_{-1,h}\geq\frac{1}{\mathcal{M}}\|\chi\|_{-1,h}^2-\frac{1}{\mathcal{M}}\left\|\varphi_h^{m-1}\right\|_{-1,h}^2.$$

Invoking Lemma 2.1 yields,

$$2\lambda\tau\,a_h^{IP}\left(\chi,\chi\right)\geq2C_{coer}\lambda\tau\|\chi\|_{2,h}^2.$$

Furthermore, we have

$$\begin{aligned}
6\beta\tau\left((\chi+\overline{\phi_0})^5,\chi\right)&=6\beta\tau\left((\chi+\overline{\phi_0})^4(\chi+\overline{\phi_0}),\chi\right)\\
&=3\beta\tau\left((\chi+\overline{\phi_0})^4(\chi+\overline{\phi_0}),(\chi+\overline{\phi_0})+(\chi-\overline{\phi_0})\right)\\
&=3\beta\tau\left\|\chi+\overline{\phi_0}\right\|_{L^6}^6+3\beta\tau\left((\chi+\overline{\phi_0})^4,\chi^2-\overline{\phi_0}^2\right)\\
&=3\beta\tau\left\|\chi+\overline{\phi_0}\right\|_{L^6}^6+3\beta\tau\left\|(\chi+\overline{\phi_0})^2\chi\right\|_{L^2}^2\\
&\quad-3\beta\tau\left((\chi+\overline{\phi_0})^4,\overline{\phi_0}^2\right)\\
&\geq3\beta\tau\left\|\chi+\overline{\phi_0}\right\|_{L^6}^6+3\beta\tau\left\|(\chi+\overline{\phi_0})^2\chi\right\|_{L^2}^2\\
&\quad-3\beta\tau|\overline{\phi_0}|^2\left\|(\chi+\overline{\phi_0})^3\right\|_{L^2}\left\|\chi+\overline{\phi_0}\right\|_{L^2}\\
&\geq3\beta\tau\left\|\chi+\overline{\phi_0}\right\|_{L^6}^6+3\beta\tau\left\|(\chi+\overline{\phi_0})^2\chi\right\|_{L^2}^2\\
&\quad-\frac{3}{4}\beta\tau\left\|(\chi+\overline{\phi_0})^3\right\|_{L^2}^2-3\beta\tau|\overline{\phi_0}|^4\left\|\chi+\overline{\phi_0}\right\|_{L^2}^2\\
&\geq\frac{9}{4}\beta\tau\left\|\chi+\overline{\phi_0}\right\|_{L^6}^6+3\beta\tau\left\|(\chi+\overline{\phi_0})^2\chi\right\|_{L^2}^2\\
&\quad-3\beta\tau|\overline{\phi_0}|^4C_{P,1}\left\|\chi+\overline{\phi_0}\right\|_{2,h}^2\\
&=\frac{9}{4}\beta\tau\left\|\chi+\overline{\phi_0}\right\|_{L^6}^6+3\beta\tau\left\|(\chi+\overline{\phi_0})^2\chi\right\|_{L^2}^2\\
&\quad-3\beta\tau|\overline{\phi_0}|^4C_{P,1}\|\chi\|_{2,h}^2,
\end{aligned}$$

where $C_{P,1}$ is a constant only depending upon the Poincaré constant (13). Thus,

$$\begin{aligned}(\mathscr{G}_h(\chi),\chi) =\ & 6\beta\tau\left((\chi+\overline{\phi_0})^5-(\varphi_h^{m-1}+\overline{\phi_0})^3,\chi\right)+2\tau\left((\chi+\overline{\phi}_0)|\nabla\varphi_h^{m-1}|^2,\chi\right)\\ &+2\tau\left((\chi+\overline{\phi}_0)^2\nabla\chi,\nabla\chi\right)-2a_0\tau\left(\nabla\varphi_h^{m-1},\nabla\chi\right)\\ &+2\tau\lambda\, a_h^{IP}\left(\chi,\chi\right)+\frac{2}{\mathcal{M}}\left(\chi-\varphi_h^{m-1},\chi\right)_{-1,h}\\ \geq\ & \frac{1}{\mathcal{M}}\left\|\chi\right\|_{-1,h}^2+\tau\left(C_{coer}\lambda-3\beta|\overline{\phi_0}|^4C_{P,1}\right)\left\|\chi\right\|_{2,h}^2\\ &-\Big(\frac{2C_P^4\tau^2}{C_{coer}\lambda}\left\|3\beta\left(\varphi_h^{m-1}+\overline{\phi_0}\right)^3-\overline{\phi}_0|\nabla\varphi_h^{m-1}|^2\right\|_{L^2}^2\\ &+\frac{2C_P^2a_0^2\tau^2}{C_{coer}\lambda}\left\|\varphi_h^{m-1}\right\|_{L^2}^2+\frac{1}{\mathcal{M}}\left\|\varphi_h^{m-1}\right\|_{-1,h}^2\Big)\geq 0,\end{aligned}$$

for $\|\chi\|_{-1,h}=q$ where

$$\begin{aligned}q^2=\ & \frac{2\mathcal{M}C_P^4\tau^2}{C_{coer}\lambda}\left\|3\beta\left(\varphi_h^{m-1}+\overline{\phi}_0\right)^3-\overline{\phi}_0|\nabla\varphi_h^{m-1}|^2\right\|_{L^2}^2+\frac{2\mathcal{M}C_P^2a_0^2\tau^2}{C_{coer}\lambda}\left\|\varphi_h^{m-1}\right\|_{L^2}^2\\ &+\left\|\varphi_h^{m-1}\right\|_{-1,h}^2\end{aligned}$$

and $\lambda\geq\dfrac{3\beta|\overline{\phi}_0|^4C_{P,1}}{C_{coer}}$. □

3.2. Unconditional Energy Stability. To show unconditional energy stability with respect to a discrete energy law, we begin by defining a discrete energy closely related to (1),

(26)
$$F(\phi):=\frac{\beta}{2}\left\|\phi\right\|_{L^6}^6-\frac{3\beta}{4}\left\|\phi\right\|_{L^4}^4+\frac{\beta|\Omega|}{4}+\frac{1}{2}\left\|\phi\nabla\phi\right\|_{L^2}^2-\frac{a_0}{2}\left\|\nabla\phi\right\|_{L^2}^2+\frac{\lambda}{2}a_h^{IP}\left(\phi,\phi\right).$$

Lemma 3.2. *Let $(\phi_h^m,\mu_h^m)\in Z_h\times V_h$ be a solution of (21). Then the following energy law holds for any $h,\tau>0$:*

$$F\left(\phi_h^\ell\right)+\tau\sum_{m=1}^{\ell}\left\|\sqrt{\mathcal{M}}\nabla\mu_h^m\right\|_{L^2}^2\leq F\left(\phi_h^0\right), \tag{27}$$

for all $1\leq\ell\leq M$.

Proof. Setting $\nu=\mu_h^m$ in (6a) and $\psi=\delta_\tau\phi_h^m$ in (6b), we have

$$\begin{aligned}(\delta_\tau\phi_h^m,\mu_h^m)+(\mathcal{M}\nabla\mu_h^m,\nabla\mu_h^m)=0,\\ 3\beta\left((\phi_h^m)^5-(\phi_h^{m-1})^3,\delta_\tau\phi_h^m\right)+\left((\phi_h^m)^2\nabla\phi_h^m,\nabla\delta_\tau\phi_h^m\right)+\left(\phi_h^m|\nabla\phi_h^{m-1}|^2,\delta_\tau\phi_h^m\right)\\ -a_0\left(\nabla\phi_h^{m-1},\nabla\delta_\tau\phi_h^m\right)+\lambda\, a_h^{IP}\left(\phi_h^m,\delta_\tau\phi_h^m\right)-\left(\mu_h^m,\delta_\tau\phi_h^m\right)=0\end{aligned}$$

Adding the two equations together, we obtain

$$\begin{aligned}&\left\|\sqrt{\mathcal{M}}\nabla\mu_h^m\right\|_{L^2}^2+3\beta\left((\phi_h^m)^5-(\phi_h^{m-1})^3,\delta_\tau\phi_h^m\right)+\left((\phi_h^m)^2\nabla\phi_h^m,\nabla\delta_\tau\phi_h^m\right)\\ &+\left(\phi_h^m|\nabla\phi_h^{m-1}|^2,\delta_\tau\phi_h^m\right)-\ a_0\left(\nabla\phi_h^{m-1},\nabla\delta_\tau\phi_h^m\right)+\lambda\, a_h^{IP}\left(\phi_h^m,\delta_\tau\phi_h^m\right)=0.\end{aligned} \tag{28}$$

Now, using a Taylor series expansion, we have

$$\begin{aligned}(\phi_h^m)^5\delta_\tau\phi_h^m&=\frac{1}{6\tau}\left((\phi_h^m)^6-(\phi_h^{m-1})^6\right)+\frac{5}{2\tau}(\xi_h)^4(\phi^{m-1}-\phi_h^m)^2\\ (\phi_h^{m-1})^3\delta_\tau\phi_h^m&=\frac{1}{4\tau}\left((\phi_h^m)^4-(\phi_h^{m-1})^4\right)-\frac{3}{2\tau}(\eta_h)^2(\phi^m-\phi_h^{m-1})^2,\end{aligned} \tag{29}$$

where ξ_h, η_h are between ϕ_h^{m-1} and ϕ_h^m. Therefore,

$$3\beta\left((\phi_h^m)^5-(\phi_h^{m-1})^3,\delta_\tau\phi_h^m\right)\geq\frac{\beta}{2\tau}\left(\|\phi_h^m\|_{L^6}^6-\left\|\phi_h^{m-1}\right\|_{L^6}^6\right)$$
$$-\frac{3\beta}{4\tau}\left(\|\phi_h^m\|_{L^4}^4-\left\|\phi_h^{m-1}\right\|_{L^4}^4\right). \tag{30}$$

Additionally, by the polarization identity, we have

$$\begin{aligned}&\left((\phi_h^m)^2\nabla\phi_h^m,\nabla\delta_\tau\phi_h^m\right)+\left(\phi_h^m|\nabla\phi_h^{m-1}|^2,\delta_\tau\phi_h^m\right)\\&\quad=\frac{1}{2\tau}\left((\phi_h^m)^2,|\nabla\phi_h^m|^2-|\nabla\phi_h^{m-1}|^2+|\nabla\phi_h^m-\nabla\phi_h^{m-1}|^2\right)\\&\qquad+\frac{1}{2\tau}\left(|\nabla\phi_h^{m-1}|^2,(\phi_h^m)^2-(\phi_h^{m-1})^2+(\phi_h^m-\phi_h^{m-1})^2\right)\\&\quad\geq\frac{1}{2\tau}\left(\|\phi_h^m\nabla\phi_h^m\|_{L^2}^2-\left\|\phi_h^{m-1}\nabla\phi_h^{m-1}\right\|_{L^2}^2\right),\end{aligned} \tag{31}$$

$$\begin{aligned}a_0\left(\nabla\phi_h^{m-1},\nabla\delta_\tau\phi_h^m\right)&=\frac{a_0}{2\tau}\left(\|\nabla\phi_h^m\|_{L^2}^2-\left\|\nabla\phi_h^{m-1}\right\|_{L^2}^2-\left\|\nabla\phi_h^m-\nabla\phi_h^{m-1}\right\|_{L^2}^2\right)\\&\leq\frac{a_0}{2\tau}\left(\|\nabla\phi_h^m\|_{L^2}^2-\left\|\nabla\phi_h^{m-1}\right\|_{L^2}^2\right)\end{aligned}$$

which implies that

$$-a_0\left(\nabla\phi_h^{m-1},\nabla\delta_\tau\phi_h^m\right)\geq-\frac{a_0}{2\tau}\left(\|\nabla\phi_h^m\|_{L^2}^2-\left\|\nabla\phi_h^{m-1}\right\|_{L^2}^2\right) \tag{32}$$

and, finally,

$$\begin{aligned}&a_h^{IP}\left(\phi_h^m,\delta_\tau\phi_h^m\right)=\\&\frac{1}{2\tau}\left(a_h^{IP}\left(\phi_h^m,\phi_h^m\right)-a_h^{IP}\left(\phi_h^{m-1},\phi_h^{m-1}\right)+a_h^{IP}\left(\phi_h^m-\phi_h^{m-1},\phi_h^m-\phi_h^{m-1}\right)\right)\\&\geq\frac{1}{2\tau}\left(a_h^{IP}\left(\phi_h^m,\phi_h^m\right)-a_h^{IP}\left(\phi_h^{m-1},\phi_h^{m-1}\right)\right).\end{aligned} \tag{33}$$

Combining (28), (30), (31), (32), and (33) and applying $\tau\sum_{m=1}^{\ell}$ gives the desired result. □

The discrete energy law immediately implies the following uniform *a priori* estimates for ϕ_h^m and μ_h^m.

Lemma 3.3. *Let $(\phi_h^m,\mu_h^m)\in Z_h\times V_h$ be a solution of (21). Suppose that $F(\phi_h^0)\leq C$ independent of h and that $\lambda>\max\left\{\frac{3\beta|\overline{\phi}_0|^4C_{P,1}}{C_{coer}},\frac{a_0C_{P,2}}{C_{coer}}\right\}>0$ where $C_{P,1},C_{P,2}$ are constants only depending upon the Poincaré constant (13) and do not depend on h or τ. Then the following estimates hold for any $\tau,h>0$:*

$$\max_{0\leq m\leq M}\left[\|\phi_h^m\|_{L^2}^2+\|\nabla\phi_h^m\|_{L^2}^2+\|\phi_h^m\nabla\phi_h^m\|_{L^2}^2+\|\phi_h^m\|_{2,h}^2\right]\leq C^*, \tag{34}$$

$$\tau\sum_{m=1}^{\ell}\left\|\sqrt{\mathcal{M}}\nabla\mu_h^m\right\|_{L^2}^2\leq C, \tag{35}$$

for some constant C that is independent of h,τ, and T.

Proof. The proof follows as a result of Lemmas 2.1 and 3.2 and the Poincaré type inequality (13) since

$$\begin{aligned}
&\frac{\beta}{2}\int_\Omega (\phi_h^\ell-1)^2\left((\phi_h^\ell)^2+0.5\right)(\phi_h^\ell+1)^2\,dx+\frac{1}{2}\left\|\phi_h^\ell\nabla\phi_h^\ell\right\|_{L^2}^2\\
&\quad+\left(\frac{\lambda C_{coer}}{2}-\frac{a_0C_{P,2}}{2}\right)\left\|\phi_h^\ell\right\|_{2,h}^2+\tau\sum_{m=1}^{\ell}\left\|\sqrt{\mathcal{M}}\nabla\mu_h^m\right\|_{L^2}^2\\
&\leq\frac{\beta}{2}\int_\Omega (\phi_h^\ell-1)^2\left((\phi_h^\ell)^2+0.5\right)(\phi_h^\ell+1)^2\,dx+\frac{1}{2}\left\|\phi_h^\ell\nabla\phi_h^\ell\right\|_{L^2}^2\\
&\quad+\frac{\lambda}{2}a_h^{IP}\left(\phi_h^\ell,\phi_h^\ell\right)-\frac{a_0}{2}\left\|\nabla\phi_h^\ell\right\|_{L^2}^2+\tau\sum_{m=1}^{\ell}\left\|\sqrt{\mathcal{M}}\nabla\mu_h^m\right\|_{L^2}^2\\
&=\frac{\beta}{2}\left\|\phi_h^\ell\right\|_{L^6}^6-\frac{3\beta}{4}\left\|\phi_h^\ell\right\|_{L^4}^4+\frac{\beta|\Omega|}{4}+\frac{1}{2}\left\|\phi_h^\ell\nabla\phi_h^\ell\right\|_{L^2}^2-\frac{a_0}{2}\left\|\nabla\phi_h^\ell\right\|_{L^2}^2+\frac{\lambda}{2}a_h^{IP}\left(\phi_h^\ell,\phi_h^\ell\right)\\
&\quad+\tau\sum_{m=1}^{\ell}\left\|\sqrt{\mathcal{M}}\nabla\mu_h^m\right\|_{L^2}^2\\
&=F\left(\phi_h^\ell\right)+\tau\sum_{m=1}^{\ell}\left\|\sqrt{\mathcal{M}}\nabla\mu_h^m\right\|_{L^2}^2\leq F\left(\phi_h^0\right)\leq C
\end{aligned}$$

for $\lambda>\max\left\{\dfrac{3\beta|\overline{\phi}_0|^4C_{P,1}}{C_{coer}},\dfrac{a_0C_{P,2}}{C_{coer}}\right\}>0$ and any $0\leq\ell\leq M$. □

3.3. Uniqueness of the Solution. We are now in a position to prove that the solution to (21) is unique.

Lemma 3.4. *Let $\phi_h^{m-1}\in Z_h$ be given and*

$$\lambda>\max\left\{\frac{3\beta|\overline{\phi}_0|^4C_{P,1}}{C_{coer}},\frac{a_0C_{P,2}}{C_{coer}},\frac{C^*C_{P,3}}{C_{coer}}\right\}>0,$$

where C^* is the constant from (34) *and $C_{P,1},C_{P,2},C_{P,3}$ are all constants depending only upon the Poincaré constant* (13) *and do not depend on h or τ. Then, the solution to* (21) *is unique for all $h,\tau>0$.*

Proof. Let $\phi_h^{m-1}\in Z_h$ be given and let $(\phi_h^m,\mu_h^m)\in Z_h\times V_h$ and $(\Phi_h^m,\mathsf{M}_h^m)\in Z_h\times V_h$ be two sets of solutions to (21). Then, it follows that for all $\nu_h\in V_h$ and all $\psi_h\in Z_h$

$$(\delta_\tau\phi_h^m-\delta_\tau\Phi_h^m,\nu_h)+(\mathcal{M}\nabla(\mu_h^m-\mathsf{M}_h^m),\nabla\nu_h)=0, \tag{36a}$$

$$\begin{aligned}
&3\beta\left((\phi_h^m)^5-(\Phi_h^m)^5,\psi_h\right)+\left((\phi_h^m-\Phi_h^m)|\nabla\phi_h^{m-1}|^2,\psi_h\right)+\lambda\,a_h^{IP}\left(\phi_h^m-\Phi_h^m,\psi_h\right)\\
&\quad+\left((\phi_h^m)^2\nabla\phi_h^m-(\Phi_h^m)^2\nabla\Phi_h^m,\nabla\psi_h\right)-(\mu_h^m-\mathsf{M}_h^m,\psi_h)=0.
\end{aligned} \tag{36b}$$

Setting $\nu_h=\frac{\tau}{\mathcal{M}}\mathsf{T}_h(\delta_\tau\phi_h^m-\delta_\tau\Phi_h^m)$ in (36a) and $\psi_h=\phi_h^m-\Phi_h^m$ in (36b), we obtain

$$\begin{aligned}
&3\beta\tau\left((\phi_h^m)^5-(\Phi_h^m)^5,\phi_h^m-\Phi_h^m\right)+\tau\left((\phi_h^m-\Phi_h^m)|\nabla\phi_h^{m-1}|^2,\phi_h^m-\Phi_h^m\right)\\
&\quad+\tau\left((\phi_h^m)^2\nabla\phi_h^m-(\Phi_h^m)^2\nabla\Phi_h^m,\nabla(\phi_h^m-\Phi_h^m)\right)\\
&\qquad+\tau\lambda\,a_h^{IP}\left(\phi_h^m-\Phi_h^m,\phi_h^m-\Phi_h^m\right)+\frac{1}{\mathcal{M}}\left(\phi_h^m-\Phi_h^m,\phi_h^m-\Phi_h^m\right)_{-1,h}=0.
\end{aligned}$$

Using the fact that

$$\begin{aligned}\left(a^5-b^5,a-b\right) &= \left((a-b)(a^4+a^3b+a^2b^2+ab^3+b^4),a-b\right)\\ &= \left((a-b)\left(\frac{1}{4}(a+b)^4+\frac{1}{4}(a^4+b^4)+\frac{1}{2}(a^2-b^2)^2+\frac{1}{2}a^2b^2\right),a-b\right)\\ &\geq \left(\frac{1}{4}(a^4+b^4)(a-b),(a-b)\right)\\ &\geq \frac{1}{4}\left(a-b,a-b\right)=\frac{1}{4}\left\|a-b\right\|_{L^2}^2\end{aligned}$$

along with Lemma 2.1, we have

$$\begin{aligned}&\frac{3}{4}\beta\tau\ \left\|\phi_h^m-\Phi_h^m\right\|_{L^2}^2+\tau\left\|(\phi_h^m-\Phi_h^m)\nabla\phi_h^{m-1}\right\|_{L^2}^2+C_{coer}\lambda\tau\left\|\phi_h^m-\Phi_h^m\right\|_{2,h}^2\\ &\qquad+\frac{1}{\mathcal{M}}\left\|\phi_h^m-\Phi_h^m\right\|_{-1,h}^2+\frac{\tau}{3}\left(\nabla\left((\phi_h^m)^3-(\Phi_h^m)^3\right),\nabla(\phi_h^m-\Phi_h^m)\right)\leq 0.\end{aligned}$$

An application of the product rule along with the fact that $a^3-b^3=(a-b)(a^2+ab+b^2)$ leads to

$$\begin{aligned}&\frac{3}{4}\beta\tau\ \left\|\phi_h^m-\Phi_h^m\right\|_{L^2}^2+\tau\left\|(\phi_h^m-\Phi_h^m)\nabla\phi_h^{m-1}\right\|_{L^2}^2+C_{coer}\lambda\tau\left\|\phi_h^m-\Phi_h^m\right\|_{2,h}^2\ +\\ &\frac{1}{\mathcal{M}}\left\|\phi_h^m-\Phi_h^m\right\|_{-1,h}^2+\frac{\tau}{3}\left(\left((\phi_h^m)^2+\phi_h^m\Phi_h^m+(\Phi_h^m)^2\right)\nabla\left(\phi_h^m-\Phi_h^m\right),\nabla(\phi_h^m-\Phi_h^m)\right)\\ &+\frac{\tau}{3}\left(\left(\phi_h^m-\Phi_h^m\right)\nabla\left((\phi_h^m)^2+\phi_h^m\Phi_h^m+(\Phi_h^m)^2\right),\nabla\left(\phi_h^m-\Phi_h^m\right)\right)\leq 0.\end{aligned}$$

Additionally, since $a^2+ab+b^2\geq\frac{1}{2}(a^2+b^2)\geq 0$ and ϕ_h^m and Φ_h^m are both solutions to (21), by Lemma 3.3 and Hölder's and Young's inequalities, we have

$$\begin{aligned}&\frac{3}{4}\beta\tau\ \left\|\phi_h^m-\Phi_h^m\right\|_{L^2}^2+\tau\left\|(\phi_h^m-\Phi_h^m)\nabla\phi_h^{m-1}\right\|_{L^2}^2+C_{coer}\lambda\tau\left\|\phi_h^m-\Phi_h^m\right\|_{2,h}^2\\ &\quad+\frac{1}{\mathcal{M}}\left\|\phi_h^m-\Phi_h^m\right\|_{-1,h}^2+\frac{\tau}{3}\left\|\nabla\left(\phi_h^m-\Phi_h^m\right)\right\|_{L^2}^2\\ &\qquad\leq-\frac{\tau}{3}\left(\left(\phi_h^m-\Phi_h^m\right)\nabla\left((\phi_h^m)^2+\phi_h^m\Phi_h^m+(\Phi_h^m)^2\right),\nabla\left(\phi_h^m-\Phi_h^m\right)\right)\\ &\qquad\leq\frac{\tau}{3}\left\|\nabla\left((\phi_h^m)^2+\phi_h^m\Phi_h^m+(\Phi_h^m)^2\right)\right\|_{L^2}\left\|\phi_h^m-\Phi_h^m\right\|_{L^4}\left\|\nabla\left(\phi_h^m-\Phi_h^m\right)\right\|_{L^4}\\ &\qquad\leq\frac{\tau}{2}\left\|\nabla\left((\phi_h^m)^2+(\Phi_h^m)^2\right)\right\|_{L^2}\left\|\phi_h^m-\Phi_h^m\right\|_{L^4}\left\|\nabla\left(\phi_h^m-\Phi_h^m\right)\right\|_{L^4}\\ &\qquad\leq\tau\left(\left\|\phi_h^m\nabla\phi_h^m\right\|_{L^2}+\left\|\Phi_h^m\nabla\Phi_h^m\right\|_{L^2}\right)\left\|\phi_h^m-\Phi_h^m\right\|_{L^4}\left\|\nabla\left(\phi_h^m-\Phi_h^m\right)\right\|_{L^4}\\ &\qquad\leq C^*\tau\left\|\phi_h^m-\Phi_h^m\right\|_{L^4}\left\|\nabla\left(\phi_h^m-\Phi_h^m\right)\right\|_{L^4}\\ &\qquad\leq C^*C_{P,3}\tau\left\|\phi_h^m-\Phi_h^m\right\|_{2,h},\end{aligned}$$

where C^* is the constant from the bound found in Lemma 3.3 and $C_{P,3}$ depends only upon the Poincaré type inequality and do not depend on h or τ. Choosing

$$\lambda>\max\left\{\frac{3\beta|\overline{\phi}_0|^4C_{P,1}}{C_{coer}},\frac{a_0C_{P,2}}{C_{coer}},\frac{C^*C_{P,3}}{C_{coer}}\right\}>0$$

concludes the proof. □

4. Numerical Results

In this section, we present several numerical experiments demonstrating the effectiveness of our method. All numerical experiments were completed using the Firedrake and FEniCS projects [33, 34] and fix $a_0=4$ and $\beta=5$.

4.1. Accuracy Example. In our first experiment, we set the initial conditions to be:

$$\phi(x, y) = 0.3\cos(3x) + 0.5\cos(y)$$

and solve on the domain $\Omega = [0, 2\pi]^2$ to a final stopping time of $T = 0.4$. We take $\mathscr{T}_h$ to be a regular triangulation of Ω consisting of right isosceles triangles with the coarsest mesh subdividing each side of the domain by 2. We then refine the mesh by taking a hierarchy of nested triangulations where each updated mesh is obtained by subdividing the triangles of the current mesh into four congruent sub-triangles. As source terms are not naturally present in the formulation of (21a)–(21b), an exact solution is not available. Therefore, to show first-order convergence in the energy norm, we consider the exact solution to correspond to the solution from the mesh with $N = 256$. We then compare and compute the errors between this solution and the solution found on coarser meshes. Additionally, we scale the time step size with the mesh size by $\tau = {}^{0.05}/_{N}$ and set the mobility as $\mathcal{M} = 10^{-3}$, $\lambda = 1$, and the penalty parameter $\alpha = 8$. The finite element spaces utilize P_2 Lagrange finite elements to approximate ϕ_h and P_1 Lagrange finite elements to approximate μ_h. Table 4.1 shows the errors and rates of convergence for the given choice of the parameters where N indicates the number of sub-intervals per side of Ω on the coarse mesh. We observe at least first-order convergence in the discrete $2, h$ norm of ϕ_h and second-order convergence in the L^2 norm of ϕ_h.

TABLE 4.1. Errors and convergence rates of the C0-IP method with $\mathcal{M} = 10^{-3}$, $\lambda = 1$, $h = {}^{2\sqrt{2}\pi}/_{N}$, $\tau = {}^{0.05}/_{N}$, and $\alpha = 8$.

N	$\|\phi_{256} - \phi_N\|_{2,h}$	rate	$\|\phi_{256} - \phi_N\|_{L^2}$	rate
8	6.1911	–	0.2625	–
16	1.9293	1.6045	0.0624	2.1039
32	0.5601	1.7221	0.0151	2.0685
64	0.1599	1.7516	0.0035	2.1336
128	0.0461	1.7354	0.0008	2.1887

4.2. Unconditional Stability Example. For our second numerical experiment, we track the total scaled energy evolution for time step sizes $\tau = 0.5, 0.25, 0.0125$, and 0.0625 with $\Omega := [0, 10]^2$, $T = 5$, and with the same initial conditions and choice of values for $\mathcal{M}$, λ, and α as in the first experiment. The mesh size corresponds to taking 128 sub-intervals along each side (or 6 refinements of the initial mesh described above). The results are displayed in Figure 2. The large time step sizes have been chosen to emphasize unconditional energy stability.

4.3. Microemulsions Examples. For the remainder of the numerical experiments, we demonstrate the effectiveness of our proposed scheme in capturing microemulsions. On a macroscopic level, microemulsions are a single-phase structured fluid consisting of homogeneous regions of oil and water and which form a complicated, intertwined structure made possible by the presence of the surfactant [10]. The surfactant molecules have an amphiphilic nature which is due to the fact that it contains two components: one component is hydrophilic (water-loving) and the other is lipophilic (fat-loving) [35]. The presence of the surfactant molecules enables the formation of a surfactant monolayer at the interface between the oil and water phases. It is the formation of these monolayers that gives the microemulsion

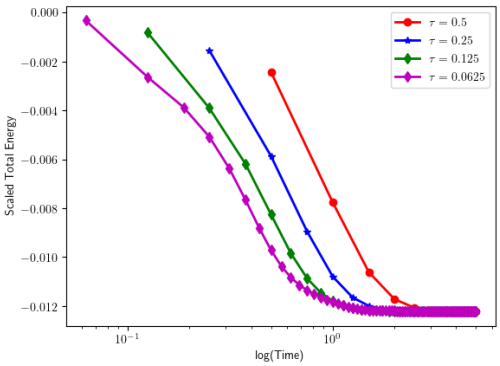

FIGURE 2. The time evolution of the scaled total energy. The mesh size is $h = {}^{10\sqrt{2}}/_{128}$, $\mathcal{M} = 10^{-3}$, $\lambda = 1$, $\alpha = 8$, τ varying as shown in the figure above, and all other parameters defined in the text.

a definite microstructure [36]. In order to demonstrate the effectiveness of our proposed scheme in capturing microemulsions, we present the results of the numerical experiments which capture the formation of this definite microstructure.

4.3.1. Microemulsions Example 1 (Replicating the profiles). For our first microemulsions experiment, the initial conditions are chosen to be randomly dispersed oil and water droplets amidst a 'continuous' surfactant media as shown in row 1, entry 1 of Figure 3 such that the initial conditions (2) are satisfied. The motivation for this experiment is derived from the numerical experiment presented in [12] in which a C^0 interior penalty finite element method was developed for (6a)–(6b) but with a different time stepping strategy than that which is presented herein. We note that the specific choice of initial conditions is not defined in [12] and, as such, our numerical experiment here is not meant as a benchmark comparison to that shown in [12]. Rather, we demonstrate that the evolution profiles look similar as both numerical methods show clear separation into oil and water regimes and capture regions of decomposition into "meandering" structures or formations of labyrinthine decomposition patterns. Here we choose $\Omega = (-5, 5)^2$ and final time $T = 0.1$. The evolution of the profiles of ϕ_h are presented in Figure 3 for $\lambda = 10^{-1}$ with $\mathcal{M} = 10^{-2}$. The experiments are performed with mesh parameters: $\tau = {}^{0.01}/_{128}$ and $h = {}^{10\sqrt{2}}/_{128}$. We observe the formation and stability of the microemulsions which is characterized by the appearance of the monolayers surrounding the pure oil and pure water phases indicated by the entries in row 3 of Figure 3. Further investigation into this relationship is an interesting direction for future research.

4.3.2. Microemulsions Example 2. For the second microemulsions experiment, we keep the same spacial domain $\Omega = (-5, 5)^2$ and the same final time $T = 0.1$ as well as the same mesh parameters: $\tau = {}^{0.01}/_{128}$ and $h = {}^{10\sqrt{2}}/_{128}$ but choose $\lambda = 10^{-1}$ and we pick larger mobility $\mathcal{M} = 10$. Initial conditions are again chosen to be a random dispersion of oil and water droplets in a 'continuous' surfactant media and these initial conditions are chosen to guarantee the satisfaction of the conditions (2). We note that the profile of the initial conditions in this experiment differs from those chosen in the above experiment. The initial conditions are displayed in row 1, entry

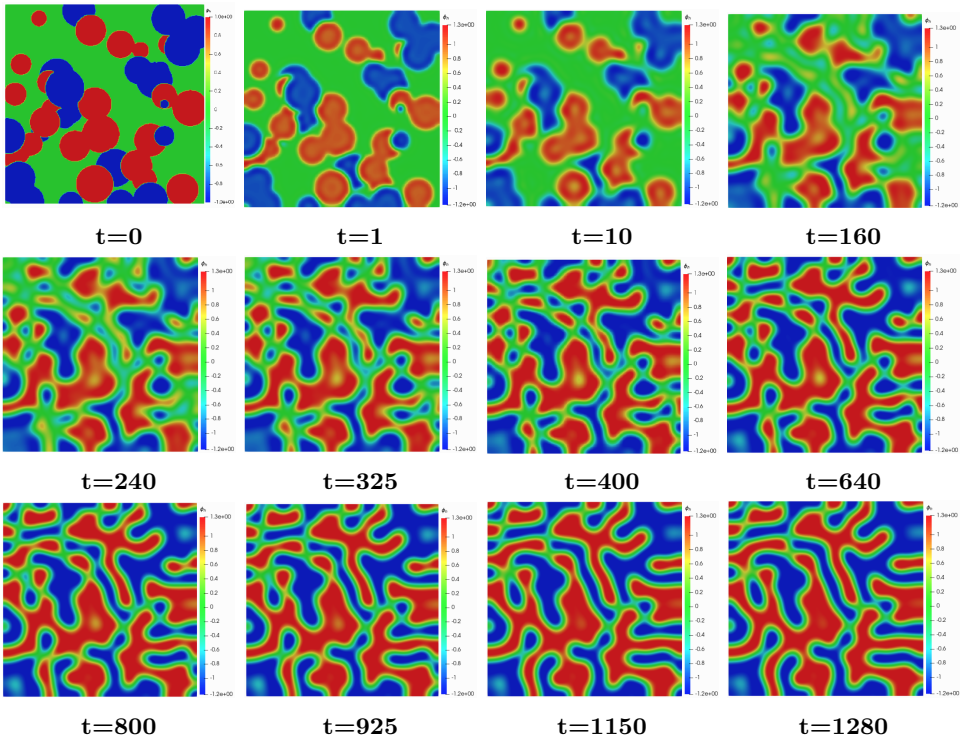

FIGURE 3. The time evolution of ϕ_h for $\lambda = 10^{-1}$, $\mathcal{M} = 10^{-2}$, $\tau = {}^{0.01}/_{128}$ and $h = {}^{10\sqrt{2}}/_{128}$.

1 of Figure 4, and the ensuing phase transition dynamics of ϕ_h are shown in the remaining snapshots present in Figure 4. Figure 4 is consistent with the previous numerical experiment in that we again observe the appearance of homogeneous regions of oil and water which form complicated, intertwined structures. However, the "meandering" regions of pure oil and pure water phases appear to have a more definite microstructure with a "thinning effect". In the next few examples, we investigate the possible cause for this effect by keeping the mobility fixed at $\mathcal{M} = 10$ and varying $\lambda = 10^{-2}, 10^{-3}$.

4.3.3. Microemulsions Example 3. For the third microemulsions experiment, we keep the same spacial domain $\Omega = (-5, 5)^2$ and the same final time $T = 0.1$ as well as the same mesh parameters: $\tau = {}^{0.01}/_{128}$ and $h = {}^{10\sqrt{2}}/_{128}$, fix the mobility at $\mathcal{M} = 10$ but choose $\lambda = 10^{-2}$. The same initial conditions as the previous experiment are considered and are displayed in row 1, entry 1 of Figure 5 with the evolution of the phases shown in the remaining snapshots of Figure 5. We notice that the decrease in λ impacts the "thinning effect" as noticed when comparing the snapshots of row 3 of Figure 5 and the snapshots of row 2 in Figure 4.

4.3.4. Microemulsions Example 4. In the fourth microemulsions experiment, we observe the phase transition dynamics by further decreasing λ to $\lambda = 10^{-3}$ with the rest of the parameters staying unchanged from the previous example. The impact of reducing λ does not result in a definite microstructure as seen in the snapshots presented in row 2 of Figure 6. We note that the lack of a definite

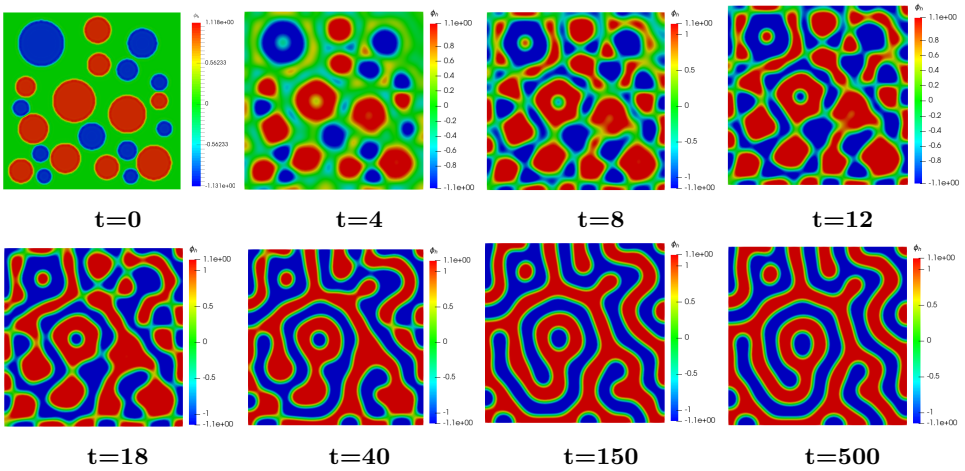

FIGURE 4. The time evolution of ϕ_h for $\lambda = 10^{-1}$, $\mathcal{M} = 10$, $\tau = {}^{0.01}/_{128}$ and $h = {}^{10\sqrt{2}}/_{128}$.

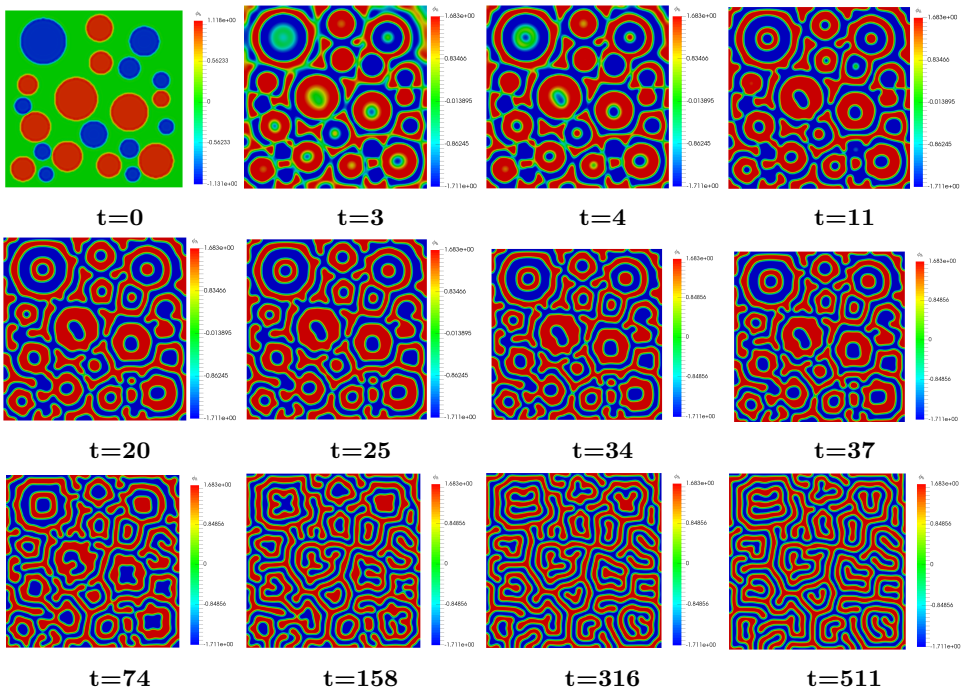

FIGURE 5. The time evolution of ϕ_h for $\lambda = 10^{-2}$, $\mathcal{M} = 10$, $\tau = {}^{0.01}/_{128}$ and $h = {}^{10\sqrt{2}}/_{128}$.

structure is likely due to the choice of λ being small enough to violate the hypothesis of Lemma 3.1.

4.4. Mass Dynamics Example. For the previous 3 experiments with fixed mobility $\mathcal{M} = 10$ but varying $\lambda = 10^{-1}, 10^{-2}, 10^{-3}$, we present the evolution of the

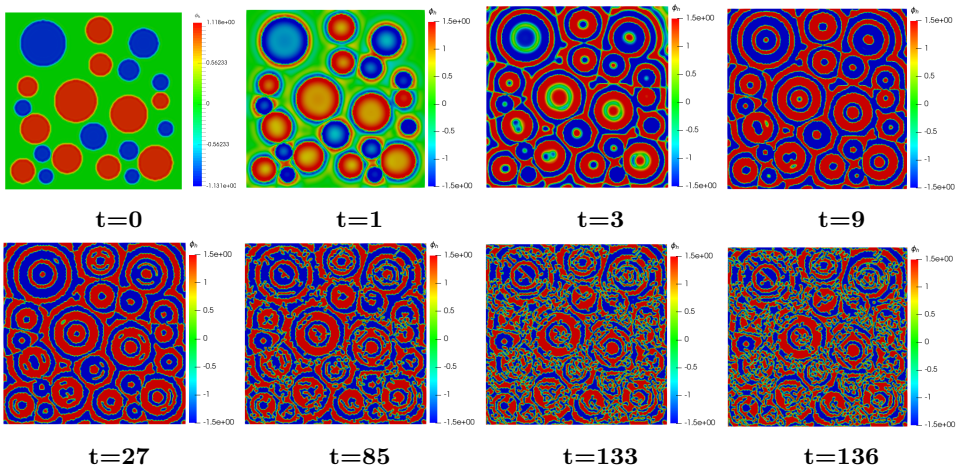

FIGURE 6. The time evolution of ϕ_h for $\lambda = 10^{-3}$, $\mathcal{M} = 10$, $\tau = {}^{0.01}/_{128}$ and $h = {}^{10\sqrt{2}}/_{128}$.

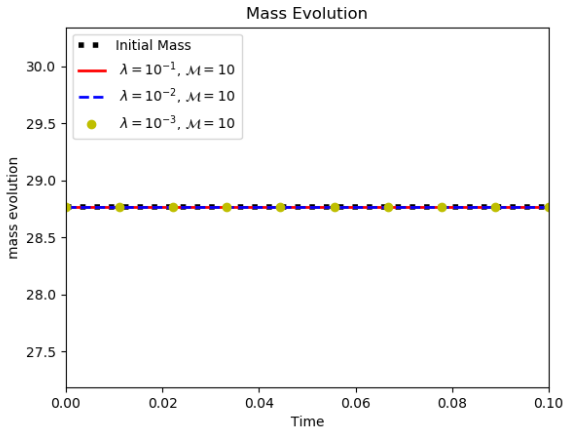

FIGURE 7. The mass dynamics in comparison to the initial mass.

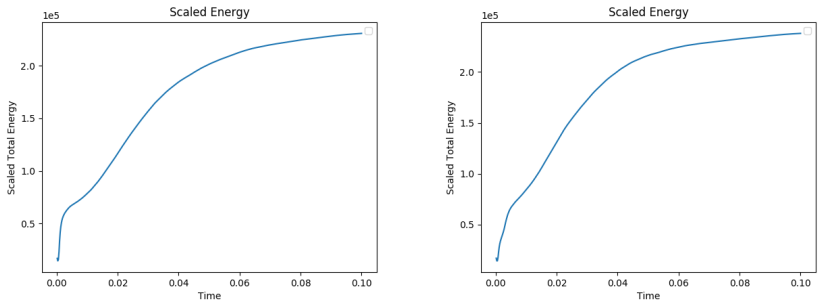

FIGURE 8. Lack of energy stability for $\lambda = 10^{-3}$ with $\mathcal{M} = 1$ *(left)* and $\mathcal{M} = 10$ *(right)*.

mass dynamics in comparison to the initial mass in Figure 7. The discrete mass conservation property is observed.

4.5. Parameter Constraint Example. We close this section by demonstrating in Figure 8 that if we take λ small enough, then we violate the hypotheses of Lemma 3.3 and we lose energy stability. This demonstrates that the conditions on λ stated in Lemma 3.3 are necessary. We take the same initial conditions, domain, mesh size, and time-step size as in the previous numerical experiment above. Specifically, we set the domain as $\Omega = (-5, 5)^2$, the final stopping time as $T = 0.1$, and the mesh parameters as $\tau = {}^{0.01}/_{128}$ and $h = {}^{10\sqrt{2}}/_{128}$. We then set $\lambda = 10^{-3}$. The energy profiles presented in Figure 8 clearly illustrate the loss of energy stability for two different choices of mobility constant, $\mathcal{M} = 1$ and $\mathcal{M} = 10$.

5. Conclusion

In this paper, we have developed an unconditionally stable numerical scheme for solving a sixth-order Cahn-Hilliard type equation that models the interfacial dynamics in ternary mixtures. We show that by using a C0 interior penalty finite element approximation for the spacial discretization and choosing a suitable temporal discretization, we have a uniquely solvable and unconditional energy stable scheme. We also demonstrate the performance of our scheme with several numerical experiments demonstrating the unconditional stability and first-order accuracy of the proposed method.

Acknowledgments

The first author AED would like to acknowledge the support of NSF Grant No. DMS-2110768. The second author NSS would like to acknowledge the support of NSF Grant No. DMS-2110774.

References

[1] Pal, B. K. and Moulik, S. P. Ionic liquid-based surfactant science: Formulation, in: Characterization and Applications, Wiley Series of Surface and 205 International Chemistry, 2015.
[2] Spinler, E. A., Zornes, Tobola, D. R., D. P. and Moradi-Araghi, A., Enhancement 200 of oil recovery using a low concentration of surfactant to improve spontaneous anf forced imbibition of chalk, in: SPE/DOE Improved Oil Recovery Symposium, Society of Petroleum Engineers, 2000.
[3] Klier, J., Tucker, C. J., Kalantar, T. H. and Green, D. P., Properties and applications of microemulsions, Adv. Mater. 12 (23) (2000) 1751-1757.
[4] Callender, S. P., Mathews, J. A., Kobernyk, K., Wettig, S. D., Microemulsion utility in pharmaceuticals: Implications for multi-drug delivery, Int J of Pharm 526 (1-2) (2017) 425-442.
[5] Gompper, G. and Goos, J., Fluctuating interfaces in microemulsion and sponge phases, Phys. Rev E 50 (2) (1994) 1325.
[6] Gompper, G. and Kraus, M., Ginzburg-Landau theory of ternary amphiphilic systems. I. Gaussian interface fluctuations, Phys. Rev. E 47 (6) (1993) 4289.
[7] Gompper, G. and Kraus, M., Ginzburg-Landau theory of ternary amphiphilic systems. II. Monte Carlo simulations, Phys. Rev. E 47 (6) (1993) 4301.
[8] Gompper, G. and Zschocke, S., Elastic proprieties of interfaces in a Ginzburg-Landau theory of swollen micelles, droplet crystals and lamellar phases, Europhys. Lett. 16 (8) (1991) 731.
[9] Gompper, G. and Zschocke, S., Ginzburg-Landau theory of oil-water-surfactant mixtures, Phys. Rev. A 46 (8) (1992) 4836.
[10] Pawłow, I. and Zajaczkowski, W., A sixth order Cahn-Hilliard type equation arising in oil-water-surfactant mixtures, Commun. Pur. Appl. Anal. 10 (2011) 1823-1847. doi:10.3934/cpaa.2011.10.1823.
[11] Schimperna, G. and Pawłow, I., On a class of Cahn-Hilliard models with nonlinear diffusion, SIAM J. Numer. Anal. 45 (1) (2013) 31-63.

[12] Hoppe, R. H. W. and Linsenmann, C. C^0-Interior Penalty Discontinuous Galerkin Approximation of a Sixth-Order Cahn-Hilliard Equation Contrib. PDEs Appl. 47 (2018) 297.
[13] Engel, G., Garikipati, K., Hughes, T. J. R., Larson,M. G., Mazzei, L. and Taylor, R. L. Continuous/discontinuous finite element approximations of fourth-order elliptic problems in structural and continuum mechanics with applications to thin beams and plates, and strain gradient elasticity, Comput. Method. Appl. M 191 (34) (2002) 3669-3750.
[14] Brenner, Susanne. C., C^0 interior penalty methods, in: Frontiers in Numerical Analysis-Durham 2010, Springer, 2011, pp. 79-147.
[15] Brenner, S. C., Gu, S., Gudi, T. and Sung, L.-Y., A Quadratic C^0 Interior Penalty Method for Linear Fourth Order Boundary Value Problems with Boundary Conditions of the Cahn–Hilliard type, SIAM J. Numer. Anal., 50 (4) (2012) 2088-2110.
[16] Brenner, S. C., Gudi, T. and Sung, L.-Y., An a posteriori error estimator for a quadratic C^0-interior penalty method for the biharmonic problem, IMA J. Numer. Anal. 30 (3) (2009) 777-798.
[17] Brenner, S. C. and Neilan, M., A C^0 interior penalty method for a fourth order elliptic singular perturbation problem, SIAM J. Numer. Anal. 49 (2) (2011) 869-892.
[18] Brenner, S. C. and Sung, L.-Y., C^0 interior penalty methods for fourth order elliptic boundary value problems on polygonal domains, J Sci. Comput. 22 (1-3) (2005) 83-118.
[19] Brenner, S. C. and Sung, L.-Y., Multigrid algorithms for C^0 interior penalty methods, SIAM J. Numer. Anal. 44 (1)(2006) 199-223.
[20] Brenner, S. C., Sung, L.-Y., Zhang, H. and Zhang, Y. A quadratic C^0 interior penalty method for the displacement obstacle problem of clamped Kirchhoff plates, SIAM J. Numer. Anal. 50 (6) (2012) 3329–3350.
[21] Brenner, S. C., Sung, L.-Y. and Zhang, Y., A quadratic C^0 interior penalty method for an elliptic optimal control problem with state constraints, Recent developments in discontinuous Galerkin finite element methods for partial differential equations, Springer, 2014, pp. 97-132.
[22] Brenner, S. C., Sung, L.-Y. and Zhang, Y., Post-processing procedures for an elliptic distributed optimal control problem with pointwise state constraints, Appl. Numer. Math. 95 (2015) 99-117.
[23] Brenner, S. C. and Wang, K., Two-level additive Schwarz preconditioners for C^0 interior penalty methods, Numer. Math. 102 (2) (2005) 231–255.
[24] Brenner, S. C., Wang, K. and Zhao, J., Poincaré–Friedrichs inequalities for piecewise H^2 functions, Numer. Func. Anal. Opt. 25 (5-6) (2004) 463-478.
[25] Fraunholz, T., Hoppe, R. H. W. and Peter, M., Convergence analysis of an adaptive interior penalty discontinuous Galerkin method for the biharmonic problem, J. Numer. Math. 23 (4) (2015) 317-330.
[26] Gudi, T., Gupta, H. S. and Nataraj N., Analysis of an interior penalty method for fourth order problems on polygonal domains, J. Sci. Comp. 54 (2013) 177-199.
[27] Guo, R.,and Xu, Y., Local discontinuous Galerkin method and high order semi-implicit scheme for the phase field crystal equation, SIAM J. Sci. Comp. 38(1), (2016) A105-27.
[28] Diegel, A. E. and Sharma, N., A C^0 Interior Penalty Method for the Phase Field Crystal Equation, Numer. Methods Partial Differ. Eq.. (2022) 1-28.
[29] Li, X. and Shen, J., Stability and error estimates of the SAV Fourier-spectral method for the Phase Field Crystal Equation, Adv. Comput. Math. 46 (2020) 1-20.
[30] Diegel, A. E. and Rebholz, L. G., Continuous data assimilation and long-time accuracy in a C0 interior penalty method for the Cahn-Hilliard equation, Appl. Math. Comput. 424 (2022) 127042.
[31] Diegel, A. E.,Feng, X. H. and Wise, S. M., Analysis of a mixed finite element method for a Cahn–Hilliard–Darcy–Stokes system, SIAM J. Numer. Anal. 53 (1) (2015) 127-152.
[32] Thomée, Vidar, Galerkin finite element methods for parabolic problems, Vol. 25, Springer & Business Media, 2007.
[33] Rathgeber, F., Ham, D. A., Mitchell L., M. Lange, M., Luporini, F., McRae, A. T. T., Bercea, G-T., Markall G. R. and Kelly, P. H. J., Firedrake: automating the finite element method by composing abstractions, ACM T. Math. Software 43 (3) (2016) 1–27.
[34] Alnæs, M., Blechta, J., Hake J., Johansson, A., Kehlet B., Logg, A., Richardson, C., Ring, J., Rognes, M. E. and G. N. Wells, The FEniCS project version 1.5, Archive of Numerical Software 3 (100).
[35] Zhang, Jianhua, Amphiphilic Molecules, Springer Berlin Heidelberg, 2016, pp. 72-75.
[36] Lee, Kai Lun, Applications and use of microemulsions, arXiv preprint arXiv:1108.2794.

[37] Yang, X. and Han, D., Linearly first-and second-order, unconditionally energy stable schemes for the Phase Field Crystal Equation, J. Comput. Phys. 330 (2017) 1116-1134.

Department of Mathematics and Statistics, Mississippi State University, Mississippi State, MS 39762
E-mail: adiegel@math.msstate.edu
URL: http://adiegel.math.msstate.edu

Department of Mathematical Sciences, University of Texas at El Paso, El Paso, TX 79968
E-mail: nssharma@utep.edu
URL: http://natasha-shilla-sharma.github.io